David P. Duda*
Hampton University, Hampton, VA 23668

Rabindra Palikonda
AS&M, Inc., Hampton, VA 23681

Patrick Minnis
Atmospheric Sciences, NASA Langley Research Center, Hampton, VA 23681

1. INTRODUCTION

Contrail-induced cloud cover has been shown to be a significant factor in regional climate change over the United States of America. As air traffic increases, the potential for globally significant impacts also rises (Minnis et al., 2004). To better understand and predict these potential climatic effects, it is necessary to develop models that can accurately represent contrail properties based on ambient atmospheric variables including temperature, relative humidity and winds.

Several high-resolution numerical weather analyses (NWA) including the 20-km Rapid Update Cycle (RUC) and the University of Oklahoma Center for Analysis and Prediction of Storms Advanced Regional Prediction System (ARPS) can provide the temperature, humidity and wind information necessary to diagnose contrail formation. One outstanding problem that must be addressed to achieve a realistic simulation of contrails is the large uncertainties in upper tropospheric relative humidity (UTH) in numerical weather analyses. Current numerical weather analyses tend to underestimate UTH due to large dry biases in the balloon soundings used to construct the analyses. To evaluate each of the models, we match several months of contrail properties derived from satellite and surface observations to the NWA-derived humidity, vertical velocity, wind shear and atmospheric stability. The relationships between several contrail properties (including optical depth and areal contrail coverage) and the NWA-derived statistics will be analyzed to determine under which atmospheric conditions widespread contrail outbreaks are favored.

2. DATA AND METHODOLOGY

2.1 Satellite Data

Multi-spectral data from the Advanced Very High Resolution Radiometer (AVHRR) onboard the *NOAA-16* satellite were used to identify linear contrails following the contrail detection algorithm of Mannstein et al. (1999). Radiance data were collected within a 4×6 degree grid box over eastern Ohio/western Pennsylvania/West Virginia (from 38° to 42°N and from 78° to 84°W) from 130 mid-afternoon overpasses of the satellite between March 2003 and July 2004 (see Fig. 1). To improve the accuracy of the automated contrail detection algorithm, the satellite overpasses were

selected based on the availability of satellite data where satellite-viewing zenith angles of all pixels are less than 50°. The visible optical depth τ of the detected contrails was computed from the contrail emissivity ε following the method of Meyer et al. (2002). Assuming a contrail temperature T_{con} of 224 K, the contrail emissivity is calculated from the 11-μm AVHRR brightness temperature T as follows

$$\varepsilon = \frac{\{B(T) - B(T_b)\}}{\{B(T_{con}) - B(T_b)\}} \qquad (1)$$

where B is the Planck function and T_b is the background temperature computed from surrounding non-contrail pixels as in Palikonda et al. (1999). The contrail longwave radiative forcing (CLRF) is calculated as in Palikonda et al. (2004).

2.2 Surface Data

Observations of contrail and cirrus occurrence and coverage across the contiguous US were collected from primary and secondary schools across the country by the Global Learning and Observations to Benefit the Environment (GLOBE) program. (See www.globe.gov for more information about the GLOBE program.) In May 2003, GLOBE initiated the contrail observation protocol to measure and classify contrail observations. A primary goal of the GLOBE program is to use detailed written protocols to enable students to provide scientifically valuable measurements of environmental parameters (Brooks and Mims, 2001). Over 14,600 observations were reported over the region between September 2003 and July 2003. They include contrail coverage, contrail number, cloud coverage, cloud type and a classification of contrails into three categories, short-lived (shrt), non-spreading persistent contrails (nspr), and spreading persistent contrails (sprd).

2.3 Meteorological Data

Meteorological data from the 20-km resolution, 1-hourly Rapid Update Cycle (RUC) analyses (Benjamin et al., 2004) and analyses from the Advanced Regional Prediction System (ARPS; see Xue et al., 2003) provide information on temperature, humidity, pressure, and vertical velocity that is matched with each of the surface and satellite observations. The ARPS data were obtained from the 27-km resolution, 1-hourly continental US domain analyses.

To match the surface and meteorological data, data from the RUC analyses closest in time with the contrail
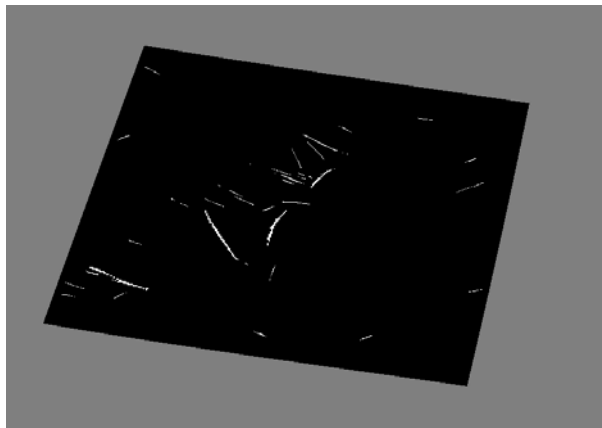
Corresponding author address: David P. Duda, NASA Langley Research Center, MS 420, Hampton, VA 23681-2199. email: d.p.duda@larc.nasa.gov.
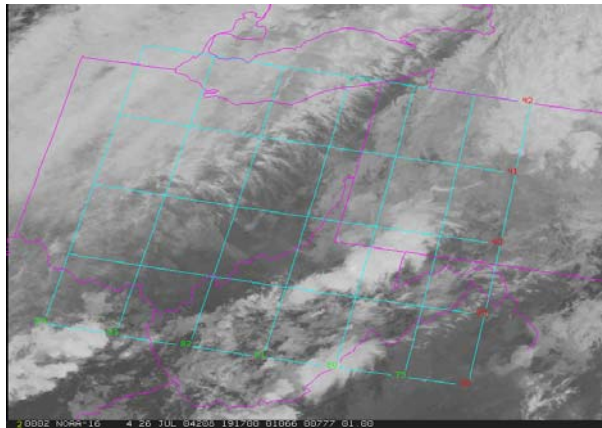
(a)
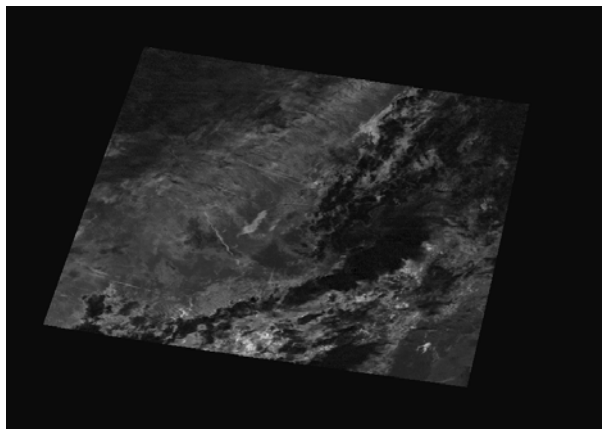
(b)

(c)

Fig. 1. (a) *NOAA-16* AVHRR channel 4 infrared (IR) imagery at 1917 UTC on 26 July 2004 showing the 4×6 degree contrail analysis region over eastern OH/western PA/WV and surrounding region (42 to 38 N; 84 to 78 W). (b) Corresponding *NOAA-16* AVHRR channel 4 minus channel 5 brightness temperature imagery highlighting contrails in grid box region shown in (a). (c) Contrails detected in grid box region using automated linear contrail detection algorithm of Mannstein et al. (1999).

observations are interpolated to the location of each observation. An observation is not used if the time difference between the surface observation and the RUC analysis was greater than 2 hours. The level between 400 and 150 hPa with the maximum relative humidity with respect to ice (RHI) is determined from all levels, spaced at every 25 hPa, having a temperature less than or equal to -40°C. Meteorological data are selected from this level for comparison with the surface observations. The temperature constraint was added to eliminate areas where the atmosphere is likely to be too warm to form contrails (Appleman, 1953). The vertical shear of the horizontal wind and the temperature lapse rate for the 25-hPa layer below the level of maximum RHI are also computed. The vertical velocity, the lapse rate (a measure of the atmospheric stability) and the vertical shear are expected to influence the spreading rate of persistent contrails (Jensen et al., 1998).

A similar procedure is used to match the ARPS upper tropospheric data with the surface-based contrail observations. The RHI is computed from the ARPS fields of potential temperature and specific humidity at the 25-hPa intervals to determine the level of maximum upper tropospheric humidity.

To compare NWA output with the satellite observations, the contrail statistics derived from the satellite imagery (contrail area, longwave radiative forcing, and contrail visible optical depth) are computed for the entire 4×6 degree grid box. Meteorological data from the RUC and ARPS are linearly interpolated to the center of each 1×1 degree box within the domain and averaged to determine mean domain values of RHI, vertical velocity, wind shear, and atmospheric lapse rate for each satellite overpass. In addition, approximately one hundred *NOAA-16* overpasses from late April through August 2004 were analyzed to correlate RHI in the 1° boxes with the occurrence of contrails and cirrus. Contrail occurrence was determined from the automated linear contrail algorithm while cirrus occurrence was determined by manual inspection of infrared imagery from each satellite overpass.

3. RESULTS
3.1 Comparison of NWA output with surface observations

Contrail coverage was reported in 24.5% of a total of 14,658 GLOBE observations. At least one persistent (either spreading or non-spreading) contrail was reported in 14.6% of the observations. Most of the persistent contrail observations (70.7%) were made in either clear skies, or skies with isolated or scattered cloudiness. Table 1 shows the mean RHI calculated from the collocated RUC and ARPS analyses for several cloudiness categories.

The increase in mean RHI with increasing cloud coverage category suggests that the GLOBE cloud and contrail observations are consistent with the NWA output, as the highest RHI values occur when overcast skies are reported. Although most persistent contrails were observed under partly cloudy conditions, the RHIs

Table 1. Mean of the maximum upper tropospheric relative humidity (%) with respect to ice (RHI) from RUC and ARPS analyses collocated with GLOBE surface observations between September 2003 and July 2004.

	RUC	ARPS
No cloud	39.24	50.69
Clear	48.94	61.36
Shrt only	52.94	65.23
Isolated	56.37	67.99
Scattered	57.85	70.65
Cirrus	61.81	75.25
Broken	63.22	77.10
Nspr only	63.90	79.19
Nspr + Sprd	65.87	80.49
Sprd only	68.08	81.86
Overcast	70.18	81.07

Table 2. Mean vertical velocity in cm s^{-1} (vv), vertical shear of the horizontal wind in m s^{-1} km^{-1} (vs), and lapse rate in K km^{-1} (lr) computed from RUC and ARPS analyses collocated with GLOBE surface observations, September 2003 - July 2004.

	vv (cm s^{-1})		vs (m s^{-1} km^{-1})		lr (K km^{-1})	
	RUC	ARPS	RUC	ARPS	RUC	ARPS
No cloud	-1.02	-0.12	3.41	2.77	-7.1	-5.9
Clear	-0.58	-0.31	3.45	3.01	-7.1	-6.3
Shrt only	+0.15	-0.32	3.02	2.89	-7.3	-6.5
Isolated	+0.19	-0.06	3.70	3.15	-7.2	-6.7
Scattered	+0.36	-0.27	3.67	3.01	-7.2	-6.8
Cirrus	+0.33	-0.13	3.79	3.12	-7.3	-7.0
Broken	+1.03	+0.12	3.72	3.21	-7.3	-7.1
Nspr only	+0.78	-0.04	3.64	3.12	-7.3	-7.1
Nspr+Sprd	+0.56	+0.21	3.45	2.96	-7.4	-7.2
Sprd only	+0.33	+0.58	3.19	2.80	-7.5	-7.4
Overcast	+2.60	+0.43	4.20	3.66	-7.3	-7.3

computed by both numerical weather analyses are higher when persistent contrails form than under usual partly cloud conditions. Table 1 shows that persistent contrails form as expected in high humidity environments, although both models show a dry bias of at least 20 to 35% when compared to contrail formation theory. The highest average RHI conditions occur with the contrail observations that include only persistent spreading contrails. The dry bias is expected as both models limit upper tropospheric moisture. Even though ice supersaturation is common in the upper troposphere and has been measured to be as high as 150% (Miloshevich et al., 2001), the RUC analyses do not allow ice supersaturation to exceed more than a few percent above 300 hPa. The ARPS analyses appear to allow some ice supersaturation, although RHI values rarely exceed 112%.

Table 2 shows the mean values of vertical velocity (vv), vertical wind shear (vs), and lapse rate (lr) from the RUC and ARPS collocated with the surface contrail observations from GLOBE. The RUC vertical velocities are slightly larger when persistent contrails are reported than under the usual partly cloudy conditions. However, the largest positive vertical velocities occur for the non-spreading contrails. For the ARPS analyses, the mean vertical velocities generally are slightly negative when skies are clear or partly cloudy, but slightly positive when persistent clouds are reported. The largest mean ARPS vertical velocities occur when only spreading persistent contrails are reported, a condition that is nearly opposite to that from the RUC.

When persistent contrails are present, the vertical shear of the horizontal wind is similar to the shear analyzed under typical partly cloudy conditions. The temperature lapse rate at the level of maximum RHI indicates the stability of the atmosphere where contrails form, and helps determine the depth of persistent contrails. Contrails will tend to be thicker as the magnitude of the lapse rate increases (i.e., the atmosphere become less stable). Table 2 shows that the largest mean lapse rates occur when spreading persistent contrails are reported.

3.2 Comparison of NWA output with satellite observations

Figure 2a shows the contrail coverage area computed for several satellite overpasses between April 2004 and July 2004 compared to the mean lapse rate in the grid box region computed by the ARPS analyses. Although the correlation between lapse rate and coverage area is poor, Fig. 2a suggests that as the lapse rate decreases (and atmospheric stability increases), the potential for large areas of spreading contrails decreases. Figure 2b compares the domain-average contrail optical depth with the domain-average RHI analyzed by the RUC for available overpasses between February 2003 and July 2004. The plot shows some correlation between optical depth and RHI, and suggests that contrail thickness is dependent on the availability of atmospheric moisture, a behavior expected from theoretical considerations.

Figure 3 presents normalized probability density histograms of RHI computed using the 1×1 degree grid boxes from the satellite overpasses. In Fig. 3a, RHI values from the RUC model are separated into grid boxes containing contrails (red dashed line) and boxes with no contrails (black solid line). The contrail distribution is skewed toward higher RHI values, but the no contrail distribution is relatively uniform. Distributions using the ARPS data are similar. The distributions in Fig 3b, which are separated by the presence or absence of cirrus, show a clear distinction in the humidity between the cirrus and non-cirrus grid boxes. This demarcation suggests that for the ARPS analyses, a simple threshold of 75% RHI would accurately predict cirrus occurrence. The results for the RUC (not shown) are similar, although the threshold between cirrus and no-cirrus is around 60 - 65%.
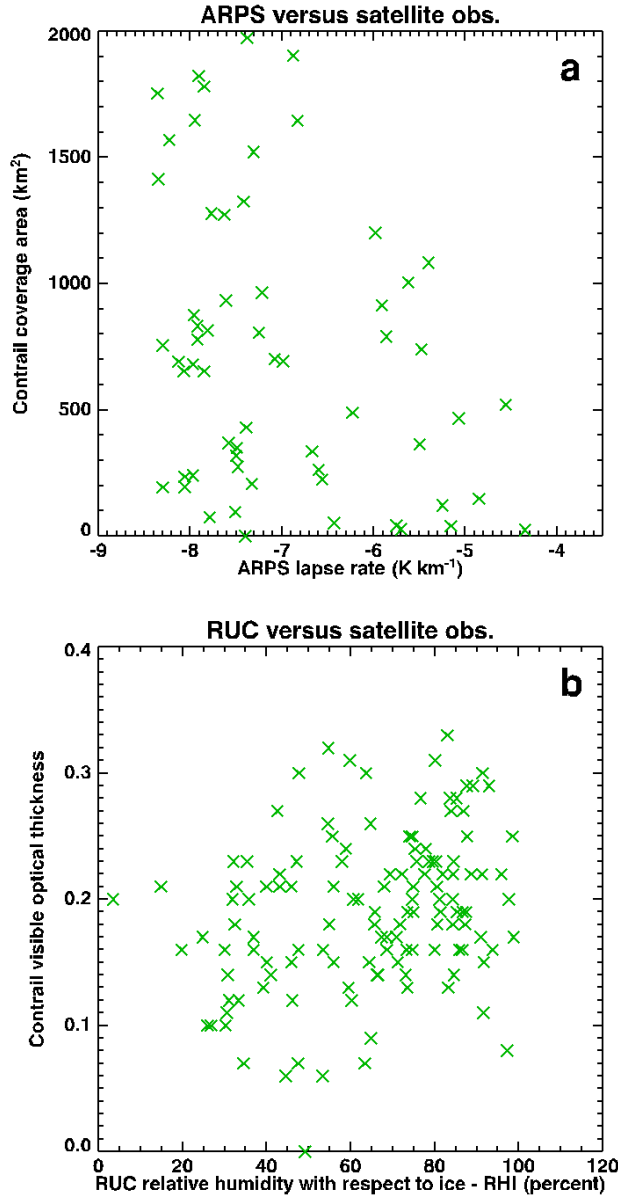
Figure 2. (a) Contrail coverage area (in km^2) estimated from NOAA-16 imagery over OH/PA/WV compared with the mean atmospheric lapse rate (in K km^{-1}) computed from ARPS analyses. **(b)** Contrail optical depth determined from NOAA-16 imagery compared with the mean RHI computed from RUC analyses.

4. DISCUSSION AND CONCLUSIONS

The results in Table 1 show that (as expected) relative humidity is the most important factor determining whether contrails are short-lived or persistent. Although most surface observations of contrails occur in clear or partly cloudy skies, the UTH observed when persistent contrails form is typically much higher than the average humidities observed under partly cloudy conditions, or when only short-lived contrails are reported. The RHI values reported when spreading contrails are observed
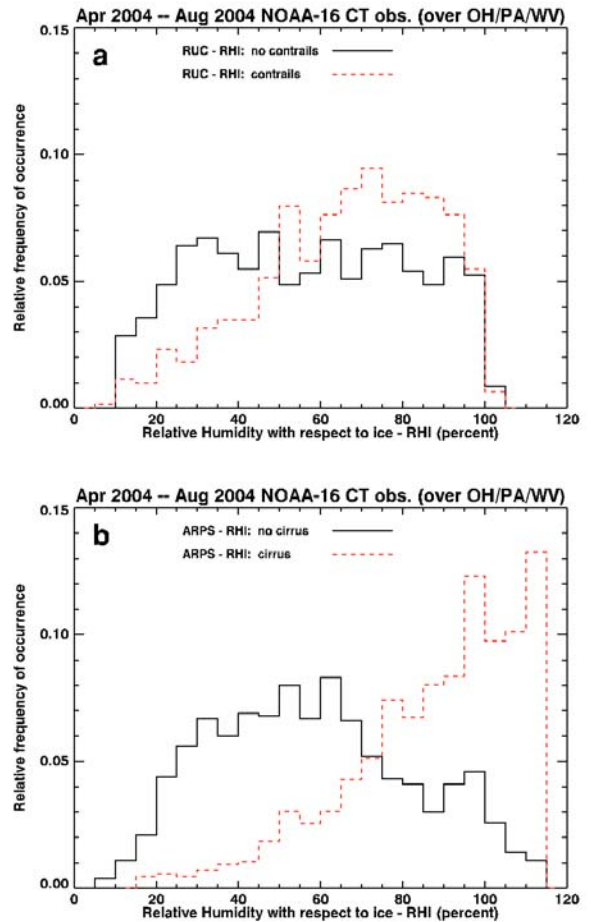

Figure 3. Contrails visually identified in *GOES-8* imagery (thick lines) and *all* flight tracks from FlyteTrax that occur in areas where the interpolated RUC model RHI at 225 hPa is greater than or equal to 85% (thin lines).

are slightly larger than when non-spreading contrails are reported, suggesting that humidity is one factor influencing the formation of spreading contrails.

Other factors including vertical velocity and the lapse rate appear to determine where spreading contrails may form. The results from the ARPS model show the clearest differences between the conditions in which non-spreading and spreading contrails are present. The spreading contrails are more likely to appear when the vertical velocities are positive than when negative, and the contrails appear to spread more when the atmosphere becomes more unstable (i.e., when the magnitude of the lapse rate increases). Although vertical wind shear is the primary mechanism responsible for the contrail spreading, it appears to be less important in determining whether contrails will spread than other factors. It is likely that sufficient UTH and atmospheric instability is necessary to make the contrails deep enough and long-lived so that the wind shear can spread the clouds. Another result of this comparison is that simple humidity thresholds in the numerical whether

analyses may be appropriate for determining where cirrus is likely to form. The prognosis of contrails from relative humidity analyses is complicated by the occasional lack of contrail formation when UTH is high. This may be the result of cirrus clouds competing with contrails for atmospheric moisture and obscuring the detection of any contrails that formed. Or, it might be due to errors in the UTH diagnosed by the models. Other factors that can affect the determination of contrails or cirrus from NWA are input data such as satellite radiances or cloud-top heights. Inclusion of those parameters could, in many instances, force the model to increase or decrease the UTH to match the observations resulting in the relatively good diagnoses of cirrus-related parameters seen here. However, such data are available only in an analysis mode and would only contribute to the diagnoses in a forecast mode indirectly by improving the forecast. Therefore, future evaluations of NWA state parameters relative to cirrus and contrails should include both model forecast and analysis datasets.

REFERENCES

Appleman, H., 1953: The formation of exhaust condensation trails by jet aircraft. *Bull. Amer. Meteor. Soc.*, **34**, 14-20.

Benjamin, S. G., D. Dévényi, S. S. Weygandt, K. J. Brundage, J. M. Brown, G. A. Grell, D. Kim, B. E. Schwartz, T. G. Smirnova, T. L. Smith, and G. S. Manikin, 2004: An hourly assimilation–forecast cycle: The RUC. *Mon. Wea. Rev.,* **132,** 495-518.

Brooks, D. R., and F. M. Mims III, 2001: Development of an inexpensive handheld LED-based Sun photometer for the GLOBE program. *J. Geophys. Res.,* **106**(D5), 4733-4740.

Jensen, E. J., A. S. Ackerman, D. E. Stevens, O. B. Toon, and P. Minnis, 1998: Spreading and growth of contrails in a sheared environment. *J. Geophys. Res.,* **103,** 31,557-31,567.

Mannstein, H., R. Meyer, and P. Wendling, 1999: Operational detection of contrails from NOAA-AVHRR data. *Intl. J. Remote Sens.,* **20,** 1641-1660.

Meyer, R., H. Mannstein, R. Meerkotter, U. Schumann and P. Wendling, 2002: Regional radiative forcing by line-shaped contrails derived from satellite data. *J.Geophys.Res.,***107**(D10),10.1029/2001JD000426.

Miloshevich, L. M., H. Vömel, A. Paukkunen, A. J. Heymsfield, and S. J. Oltmans, 2001: Characterization and correction of relative humidity measurements from Vaisala RS80-A radiosondes at cold temperatures, *J. Atmos. Oceanic Technol.,* **18,** 135-156.

Minnis, P., J. K. Ayers, R. Palikonda, and D. Phan, 2004: Contrails, cirrus trends, and climate. *J. Climate,* **17,** 1671-1683.

Palikonda, R., P. Minnis, D. R. Doelling, P. W. Heck, D. P. Duda, H. Mannstein, and U. Schumann, 1999: Potential radiative impact of contrail coverage over continental USA estimated from AVHRR data. *Proc. AMS 10th Conf. Atmos. Rad.,* Madison, WI, June 28 – Jul 2, 181-184.

Palikonda, R., P. Minnis, D. P. Duda, and H. Mannstein, 2004: Contrail coverage over the United States of America during 2001 derived from AVHRR data. *Meteorol. Z.* (submitted).

Xue, M., D.-H. Wang, J.-D. Gao, K. Brewster, and K. K. Droegemeier, 2003: The Advanced Regional Prediction System (ARPS), storm-scale numerical weather prediction and data assimilation. *Meteor. Atmos. Physics,* **82,** 139-170.